MICROWAVE PROPAGATION ATTENUATION DUE TO EARTH'S ATMOSPHERE AND WEATHER AT SHF BAND

Christian Ho, Charles Wang, Kelly Gritton and Kris Angkasa
Jet Propulsion Laboratory, California Institute of Technology
Pasadena, California 91109
Tel: 818-354-9254; email:christian.ho@jpl.nasa.gov

Abstract: *In this study we have estimated radio wave propagation losses at SHF band by applying available propagation models into several Air Force benchmark scenarios. The study shows that dominantly additional losses over the free space loss are atmospheric absorption, clouds, fog, and precipitation, as well as scintillation /multipath at low elevation angles. The free space loss equation has been modified to include all atmospheric attenuation and fading effects that cannot be neglected over the range of frequency of interest. Terrain profiles along all directions of interest within the coastal areas and inland areas for four benchmark cases have been analyzed in detail. We find that while the atmospheric gaseous absorption plays a significant role under a clear weather, heavy rainfalls can cause several tens of dB loss for a 100-km path through the rain. At very low elevation angles (< 5°), atmospheric scintillation/multipath fading becomes a very important factor. There are significant differences in the feature of anomalous mode (ducting) propagation between the east and the west coastal receiving stations.*

1. INTRODUCTION

The Department of Defense (DoD) has tasked the Advanced Range Telemetry Project (ARTP) to study the impact of augumenting some aeronautical telemetry (AT) operations from one frequency range to another. Most AT links operate in the frequency range of 1.4-2.4 GHz. The DoD is considering moving to the super high frequency (SHF) band in a range of 3-30 GHz. It is important to determine the changes to link power margins as the frequency increases. It is also necessary to identify any other propagation variances in the range of interest.

The atmospheric and weather effects on 3-30 GHz frequency band becomes more significant and is not negligible as at the 1.4-2.4 GHz frequency band which the military is using now. There are several types of attenuations which will affect the power margin at higher frequencies [1]. One is the atmospheric gaseous absorption [2], while another is the rain attenuation when microwave signals pass through the rain [3]. Additional environmental phenomena, such as, cloud [4], fog, ice, snow, aerosol, dust, etc., can also cause severer signals impairment as increasing operating frequency. Several anomalous propagation modes (such as terrain diffraction [5], ducting and tropospheric scatter [1]) also play major roles in trans-horizon interference for a very small percent time [6]. At low elevation angle, the atmospheric scintillation and multipath fading become significant [7]. A microwave propagation scenario through the atmospheric medium is shown in Figure 1. In this study, we have taken all propagation mechanisms in account.

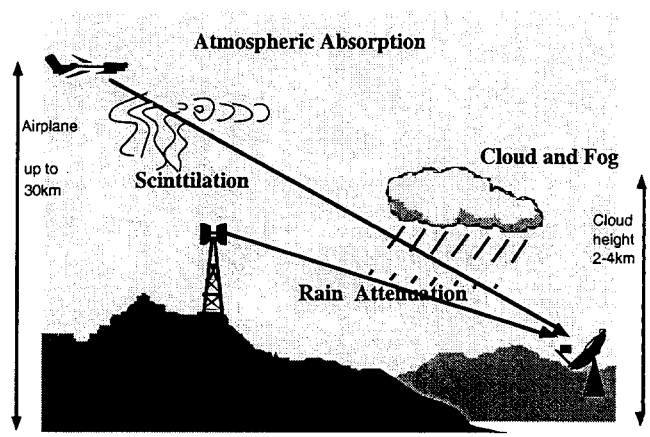

Figure 1. Microwave atmospheric propagation environment. Some typical radio paths linking aircraft to the ground and ground to ground are shown. Four types of attenuations at SHF band are shown in the Figure: Atmospheric gaseous attenuation from O_2 and condensed H_2O, rain attenuation, cloud and fog absorption and scintillation.

At first, this study will identify all major propagation mechanisms and estimate attenuation that arises in the new frequency band. Then, changes in microwave power attenuation as frequency increases from 1.4-2.4 GHz to 3-30 GHz will be determined [8, 9]. Any new propagation anomalies that might arise at some frequencies in the range of investigation have been reliably identified. As final study results, a limited set of link scenarios to serve as useful benchmark comparison paths and of benchmark weather cases that will be applied to each scenario has been established. Upper and lower

bounds on systematic and random path attenuation components at 3,6,12, 24 GHz will be estimated. In the SHF band, for the radio waves propagating through the atmospheric medium, the compensation factor to the Friis free space equation [10] need to be conservatively estimated. This study has reliably provided the estimate of upper and lower bounds on the degree to which factors currently assumed negligible such as atmospheric absorption and weather will cause additional systematic and random losses at higher frequencies.

2. BENCHMARK CASE STUDY

All microwave propagation models recommended by ITU (International Telecommunication Union) have been identified and used for this study, which include: Atmospheric absorption [2], attenuation by rainfall [3], attenuation due to clouds and fog [4], attenuation due to scintillation/multipaths [7] at low elevation angles and three anomalous propagation modes. Elevation angle dependence on propagation paths also is taken into account. These models are applied for following benchmark case scenarios.

2.1. Benchmark Case Scenarios: We have contacted the ARTM staff about available link scenarios. Four benchmark link scenarios for case study are provided as: Patuxent River, Maryland; San Nicholas Island, California; Laguna Peak, California; and Edwards Air Force Base, California.

For the first important candidate, the Naval test range at Patuxent River, Md (commonly referred to as "PAX River" or simply PAX), the primary receiving antennae are 8 foot diameter (operating 1.4-2.4 GHz) just off the Chesapeake bay, slightly inland. The antennas are approximately 80-100 feet above ground level, which is not far above sea level. The coordinates of the receiving station are: 38°18'00"N, 76°24'00"W, antenna elevation 30.5 m. An important worst case flight profile has a jet aircraft taking off and flying out to sea at altitudes that can range from 1000 to 50,000 ft and go out as far as the radio horizon.

The second benchmark location is the Navy Weapons ctr. at Pt. Mugu, CA. This West coastal operations often experience fog and ducting phenomenon. There are 2 receive antenna sites in the center. The first is on a low mountain called Laguna Peak. Antenna coordinates to use are: 34° 6' 25.79"N, 119 °3' 56.72"W , elevation 416.7m. The second antenna location is on San Nicholas Island: 33° 15' 4.50"N, 119 °31' 14.10"W, elevation 277.06m. They receive signals from all over the airspaces designated in FAA aviation sectional charts as R-2519 and W-289. In addition, they will track high-flying vehicles (missile launch) launched from Vandenburg AFB from the point at which they can first see them to the point they lose signal far out over the Pacific.

The third and final location for a case study is Edwards AFB. The main receive site is located: 34 ° 53' 36.71"N, 118 ° 0' 40.39"W, elevation of antenna #1 is 899.2m. Operations concentrate on the air spaces defined in FAA aviation sectional charts as R2508 and farther North in the "MOA" flight zones. Looking Eastward, it is not uncommon for signals to be tracked slightly beyond the Colorado river when vehicles are flying at 20k feet pressure altitude and higher.

2.2. Terrain Profile Analysis: To calculate the link budget between the stations and the neighborhood areas, we need to perform a terrain profiles analysis first [1,5]. Based the analysis, we can find whether or not the path between the transmitter and the receiver is the line of sight or trans-horizon. Radio waves are bent when they propagate through atmospheric gases that decrease in density with altitude. The waves can therefore reach locations beyond the line of sight. The severity of the bending is determined by the gradient of the refractive index near the earth's surface. It is convenient to represent the radio ray as a straight line for the sake of analysis. For this reason an "Effective Earth Radius", a_e, is defined that in effect stretches the Earth radius by a factor depending on the refractivity gradient, ΔN [11]. In this study an 4/3 earth radius has been used to modifying all terrain profiles.

Using the effective Earth radius, we can modify the elevation of terrain profile using the following equation:

$$y_i = h_i - x_i^2 / 2a_e$$

where y_i is modified elevation, h_i is terrain elevation above sea level, while x_i is distance from the receiver. The modified terrain profiles shown in Figures 2, 3, 4, 5, 6, and 7 using the median effective Earth radius. All distances and heights are referenced to these modified plots.

To construct these plots, elevations h_i of the terrain are read from topographic maps versus their distance x_i from the receiving antenna. The terrain profiles, including terrain elevations and the sea level, have been adjusted according to the average curvature of the radio ray path. The solid curve near the bottom of the figure indicates the shape of the

sea level of constant elevation ($h = 0$) for all plots. The receiving station is put at left corner, while the transmitting aircraft from the right side. The vertical scales of the figure are exaggerated in order to provide a sufficiently detailed representation of terrain irregularities.

The elevation angles θ_{er} relative to receiver may be computed using the following equations:

$$\theta_{er} = \frac{h_{Lr} - h_{rs}}{d_{Lr}} - \frac{d_{Lr}}{2a_e}$$

where h_{Lr} is the elevation of horizon obstacle and h_{rs} is elevation of receiving antennas, respectively, all above the average mean sea level (AMSL). The d_{Lr} is sea level arc distance from receiving antenna to its radio horizon obstacle.

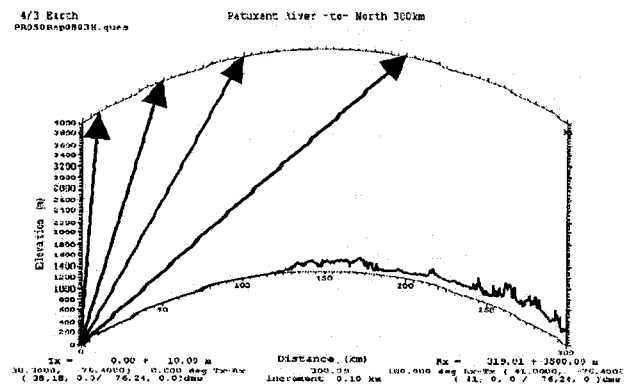

Figure 2. A modified coastal terrain profile along a 300 km path north from the Patuxent River AFB. There are a minimum elevation angle of 0.2° relative to an airplane at 4000 m altitude and a maximum 200 km path of line of sight. The Paths with 10 km, 50 km and 100 km lengths at various elevation angles are also shown.

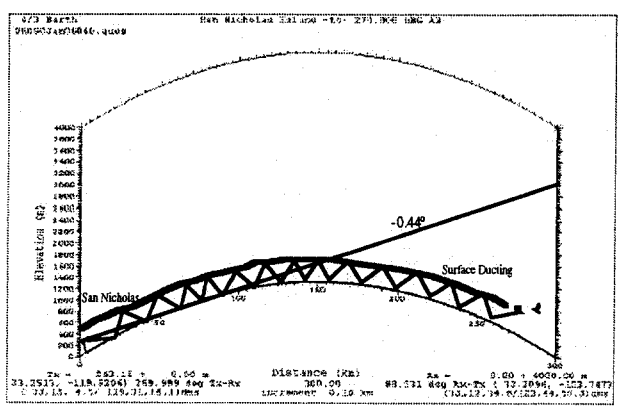

Figure 3. Terrain profile along a 300 km path west from San Nicholas Island. Relative to the receiver at San Nicholas Island, the minimum elevation angle for a line of sight in the west direction (270° azimuth) is -0.44°, corresponding to a maximum range of 65 km on the ocean surface. However, the radio signals from an aircraft can propagate beyond the horizon along a surface or elevated duct to the receiver.

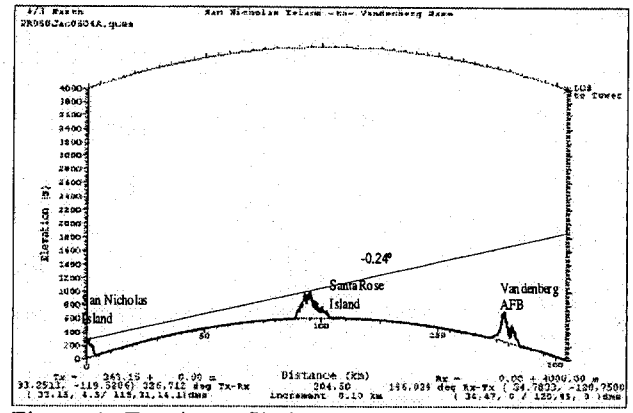

Figure 4. Terrain profile between San Nicholas Island and Vandenberg AFB. Relative to a receiver at San Nicholas Island, the minimum elevation angle in the Vandenberg direction is -0.24°. The line of sight is blocked by San Rose Island at 95 km away. However, when an aircraft arises up to 2000 m above the Vandenberg AFB, there is a direct view from the San Nicholas Island receiver.

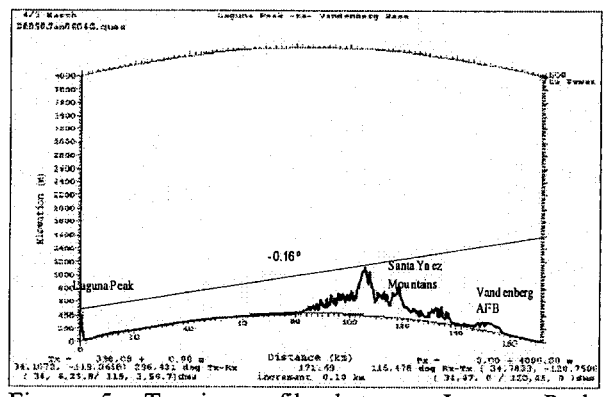

Figure 5. Terrain profile between Laguna Peak and Vandenberg AFB. The line of sight is blocked by San Ynez Mountains 110 km away, which has a -0.16° elevation angle relative to a receiver at Laguna Peak.

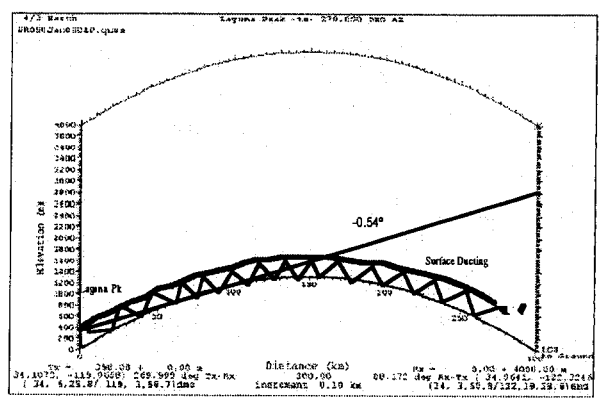

Figure 6. Terrain profile along a 300 km path west from Laguna Peak. Relative to the receiver at Laguna Peak, the minimum elevation angle for a line of sight in the west direction (270° azimuth) is -0.54°, corresponding to a maximum range of 80 km on the ocean surface. The plot shows that the radio signals from an aircraft can propagate transhorizontally along a surface or elevated duct to the receiver.

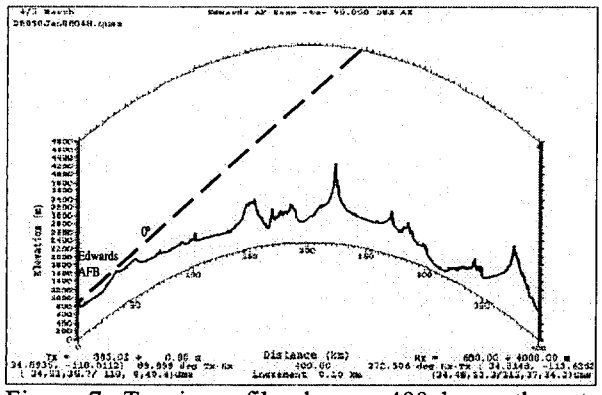

Figure 7. Terrain profile along a 400 km path east from Edwards AFB. Relative to the receiver at the base, the minimum elevation angle for a line of sight in the east direction (90° azimuth) is 0° due to a nearby hill.

2.3. Elevation Angle Dependence: Most propagation models can only apply for satellite zenith link with a total atmospheric path, instead of a limited (or partial) atmospheric path linking between the aircraft and ground . However, at most of time (98% of time) the military receivers work at below the 20° elevation angle, while 85% of time at below the 5° elevation angle, which will restrict the direct application of all types of microwave propagation models into the military communication link scenario. To solve these problems, in this study we have developed a method by scaling the total atmospheric path loss into the partial oblique path loss as shown below.

We assume that all atmospheric propagation parameters have an exponential decrease with altitude and with a vertical scale height H, that is, $A = a_0 \cdot \exp(-z/H)$, where a_0 is a coefficient and z is the vertical distance. Thus to calculate the total zenith losses through the entail atmosphere, we have a vertical loss for a partial atmospheric path, h:

$$L_h(90°) = \int_0^h a_0 \cdot \exp(-z/H)dz = a_0 H[1-\exp(-h/H)]$$

The loss for a partial oblique path (h, θ):

$$L_h(\theta) = a_0 H[1-\exp(-h\sin\theta/H)]/\sin\theta$$

Thus we have:

$$L_h(\theta) = L_\infty(\theta)[1-\exp(-h\sin\theta/H)]$$

where $L_\infty(\theta) = L_\infty(90°)/\sin\theta \quad (dB)$ and $5° \le \theta \le 90°$.

Using these equations, we can scale the total atmospheric path loss into the limited oblique path loss.

2.4. Radio Parameters and Calculation: We have applied the above method to path profile analysis for all of these four receiving stations. In order to perform the loss calculations for all types of attenuation for these locations, we need first to collect all radio climatologic parameters from these areas. We have listed all parameters in Table 1 for the four benchmark cases. These parameters are very important in accurately calculating propagation losses. We have used the following maps to make these parameters available. They are [1,2,3,4,5,6,7,11,12]:

- World map of refractive index, N, in February,
- World map of refractive index, N, in August.
- World map of vertical gradients of the radio refractive index, ΔN, in February
- World map of vertical gradients of the radio refractive index, ΔN, in August
- World map of surface water vapor density, ρ, in a unit of g/m^3 in winter
- World map of surface water vapor density, ρ, in a unit of g/m^3 in summer.
- Northern America rain zone map.
- Rain fall rates (mm/h) for various rain zones as a function of percentage of time exceeded.
- World map of normalized total columnar content of cloud liquid water (kg/m^2) exceeded for 1% of the year
- World map of normalized total columnar content of cloud liquid water (kg/m^2) exceeded for 10% of the year
- World map of surface duct occurrence rates (%) for an average year.
- World map of elevated duct occurrence rates (%) for an average year.

Based on these parameters, ll calculation results are shown in Tables 2, 3, 4 and 5 for the four benchmark cases.

By applying attenuation charts and scaling method into Patuxent River Case Study, we find that for a 50 km path with elevation angle of 6.2 degrees, the total atmospheric loss at 12.0 GHz at 1.0% of time exceeded is 8.3 dB, at 24 GHz is 34.3 dB. For a 200 km path with elevation angle of 0.2°, the total atmospheric loss at 12.0 GHz at 1.0% of time is 36.1 dB. For 24 GHz, the loss is 139.5 dB.

There are occurrence rates of 50% for elevated ducting and of 15% for surface ducting respectively, for San Nicholas Island and Laguna Peak, while both occurrence rates at Edwards AFB and Patuxent River are around 10%. This is because there are more elevated inversion layers formed over west coastal areas than over the east.

The layer height of elevated ducts at San Nicholas Island and Laguna Peak is in an altitude range from 800 m to 1000 m, while the surface duct layer can extend up to 300 m altitude. As a comparison, Edwards AFB area has smaller duct thickness.

The receiver at San Nicholas Island has a lowest elevation angle of –0.44° and a maximum line of sight range of 65 km over the ocean. In the direction of Vandenberg, the elevation angle is –0.24°. For the receiver at Laguna Peak the lowest elevation angle is –0.54° and the line of sight range is 80 km over the ocean. In the direction of Vandenberg, the elevation angle is –0.16°. However, beyond these ranges, radio signals still can propagate trans-horizontally up to ~1000 km through the anomalous ducting mode along the ocean surface.

At San Nicholas Island, total propagation losses due to gaseous absorption, rain attenuation, cloud attenuation and scintillation/multipaths (except the free space loss) for a 100-km path with 3.1° elevation angle are 12.8 dB for 12 GHz, and 49.2 dB for 24 GHz respectively. The corresponding losses at Edwards AFB are 11.0 dB and 39.2 dB respectively. This is because the west coastal area has less rain and cloud coverage when comparing with Patuxent River region (17.4 dB and 67.6 dB respectively).

3. SUMMARY OF STUDY RESULTS

In order to increase transmission bandwidth, the military aeronautical telemetry operations are upgrading their operating frequency from below 3 GHz to a range of 3-30 GHz. The present study has provided an impact assessment on microwave power link margin as operating frequency increases. Through this study we can obtain the following conclusions:

- There are four types of atmospheric losses that need to be taken into account at new SHF band.
- At high elevation angles, atmospheric gaseous absorption and rain attenuation are two dominant factors at SHF band.
- While the atmospheric gaseous absorption plays a major role under a clear weather, heavy rainfalls can cause several tens of dB loss for a 100 km path through the rain.
- Attenuations due to rain, clouds, and scintillation have strong time percentage dependences, based on the long-term statistics
- At very low elevation angles (< 5°), atmospheric scintillation/multipath fading becomes a very important factor.
- There are at least three anomalous propagation modes which can propagate trans-horizontally. These modes may be used for communication for a small percentage of time.
- There are occurrence rates of 50% for elevated ducting and of 15% for surface ducting at San Nicholas Island and Laguna Peak.
- Layers height of elevated ducts at San Nicholas Island and Laguna Peak are in an altitude range from 800 m to 1000 m, while the surface duct layer can extend up to 300 m altitude.
- San Nicholas Island has a lowest elevation angle of –0.44°, while Laguna Peak has a lowest elevation angle of –0.54° over the ocean. However, radio signals can propagate trans-horizontally up to ~1000 km through the ducting mode.
- Patuxent River has a higher total atmospheric propagation losses (except free space loss) for a 100-km path, while San Nicholas Island and Edwards AFB have less losses because of less rainfall and humidity (water vapor density).

Acknowledgements: Authors like to thank ARTM staffs at Edwards Air Force Base, California.

Reference

[1] Prediction procedure for the evaluation of microwave interference between stations on the surface of the earth at frequencies above about 0.7 GHz, Recommendation ITU-R P.452-9, 1999.
[2] Attenuation by Atmospheric Gases, Recommendation ITU-R P.676-4, 1999.
[3] Specific attenuation model for rain for use in prediction methods, ITU-R P.838, 2003.
[4] Attenuation due to clouds and fog, ITU-R P.840, 2003.
[5] Propagation by diffraction, Recommendation ITU-R P.526-8, 2003.
[6] Propagation prediction techniques and data required for the design of trans-horizon radio-relay systems, ITU-R P.617, 2003.
[7] Propagation data and prediction methods required for the design of Earth-space telecommunication systems, ITU-R P.618, 2003.
[8] Flock, W.L., Propagation effects on satellite systems at frequencies below 10 GHz, *A Handbook for Satellite Systems Design*, NASA Reference Publication 1102, 1987.
[9] Ippolito, L.J., Propagation impairments on 10 to 100 GHz satellite links with techniques for system design, *A Handbook for Satellite Systems Design*, NASA Reference Publication 1082, 1989.
[10] Calculation of free-space attenuation, ITU-R P.525, 1999.
[11] The radio refractive index: its formula and refractivity data, ITU-R P.453-9, 2001.
[12] Water vapor: Surface density and total columnar content, ITU-R P.836, 2003.

Table 1. Radio Parameters at Four Case Study Areas

Radio Parameters		**Patuxent River**	**Laguna Peak**	**San Nicholas Island**	**Edwards AFB**
Refractive Index	February	310 N-units	330 N-units	330 N-units	320 N-units
	August	360 N-units	345 N-units	350 N-units	330 N-units
Refractivity Gradient	February	40 N-units	45 N-units	45 N-units	40 N-units
	August	50 N-units	55 N-units	60 N-units	45 N-units
Water Vapor Content	February	5 g/m^3	7.0 g/m^3	7.5 g/m^3	5.5 g/m^3
	August	12 g/m^3	12 g/m^3	13 g/m^3	10 g/m^3
Rainfall Zone and Rainfall Rate	Zone	K	E	E	E
	0.1% of Time	12 mm/h	6.2 mm/h	6.2 mm/h	6.2 mm/h
	1.0% of Time	2.5 mm/h	1.8 mm/h	1.8 mm/h	1.8 mm/h
Cloud Liquid Water Columner Content	1.0% of Time	1.2 kg/m^2	0.5 kg/m^2	0.5 kg/m^2	0.4 kg/m^2
	10% of Time	0.4 kg/m^2	0.2 kg/m^2	0.2 kg/m^2	0.2 kg/m^2
Radio Climatic Zone	Inland, Coastal or Sea	A1	A1	B	A2
Ducting	Surface Duct	10%	15%	15%	10%
	Elevated Duct	10%	50%	50%	10%

Table 2. Total Propagation Losses for Typical Paths around Patuxent River

Distance (km)		Elevation Angle (Degree)	Free Space Loss (dB)	Gaseous Absorption (H_2O with 12 g/m^3)	Rain Attenuation at 1.0% of Time	Cloud Attenuation at 1.0% of Time	Scintillation /Multipath at 1.0% of Time	Total Atmospheric Attenuation (dB)	Total Attenuation (dB)
For 12.0 GHz	10	23.6	134.1	0.2	0.6	0.5	0.2	1.5	135.6
	50	6.2	148.1	2.0	3.0	1.9	1.4	8.3	156.3
	100	3.1	154.1	4.0	6.0	3.8	3.6	17.4	171.5
	200	0.2	160.1	8.0	12.0	7.50	8.6	36.1	196.2
For 24.0 GHz	10	23.6	140.1	1.6	3.2	1.0	0.4	6.2	146.3
	50	6.2	154.1	9.0	17.5	5.0	2.8	34.3	188.4
	100	3.1	160.1	18.0	35.0	10.0	4.6	67.6	227.3
	200	0.2	166.1	36.0	70.0	20.0	13.5	139.5	305.6

Table 3. Total Propagation Losses for Typical Paths around San Nicholas Island

Distance (km)		Elevation Angle (Degree)	Free Space Loss (dB)	Gaseous Absorption (H_2O with 13 g/m^3)	Rain Attenuation at 1.0% of Time	Cloud Attenuation at 1.0% of Time	Scintillation /Multipath at 1.0% of Time	Total Atmospheric Attenuation (dB)	Total Attenuation (dB)
For 12.0 GHz	10	23.6	134.1	0.2	0.4	0.2	0.2	1.0	135.1
	50	6.2	148.1	2.2	1.6	0.8	1.4	6.0	154.1
	100	3.1	154.1	4.4	3.2	1.6	3.6	12.8	166.9
	200	0.2	160.1	8.8	6.4	3.1	8.6	26.9	187.0
For 24.0 GHz	10	23.6	140.1	1.9	1.8	0.4	0.4	4.5	144.6
	50	6.2	154.1	10.7	9.2	2.1	2.8	24.8	178.9
	100	3.1	160.1	21.4	19.0	4.2	4.6	49.2	209.3
	200	0.2	166.1	42.7	38.0	8.3	13.5	102.5	268.6

Table 4. Total Propagation Losses for Typical Paths around Laguna Peak

Distance (km)		Elevation Angle (Degree)	Free Space Loss (dB)	Gaseous Absorption (H_2O with 12 g/m^3)	Rain Attenuation at 1.0% of Time	Cloud Attenuation at 1.0% of Time	Scintillation /Multipath at 1.0% of Time	Total Atmospheric Attenuation (dB)	Total Attenuation (dB)
For 12.0 GHz	10	23.6	134.1	0.2	0.4	0.2	0.2	1.0	135.1
	50	6.2	148.1	2.0	1.6	0.8	1.4	5.8	153.9
	100	3.1	154.1	4.0	3.2	1.6	3.6	12.4	166.5
	200	0.2	160.1	8.0	6.4	3.1	8.6	26.1	186.2
For 24.0 GHz	10	23.6	140.1	1.6	1.8	0.4	0.4	4.2	144.3
	50	6.2	154.1	9.0	9.2	2.1	2.8	23.1	177.2
	100	3.1	160.1	18.0	19.0	4.2	4.6	45.8	205.9
	200	0.2	166.1	36.0	38.0	8.3	13.5	95.8	261.9

Table 5. Total Propagation Losses for Typical Paths around Edwards AFB

Distance (km)		Elevation Angle (Degree)	Free Space Loss (dB)	Gaseous Absorption (H_2O with 10 g/m^3)	Rain Attenuation at 1.0% of Time	Cloud Attenuation at 1.0% of Time	Scintillation /Multipath at 1.0% of Time	Total Atmospheric Attenuation (dB)	Total Attenuation (dB)
For 12.0 GHz	10	23.6	134.1	0.2	0.3	0.2	0.2	0.9	135.0
	50	6.2	148.1	1.6	1.4	0.6	1.4	5.0	153.1
	100	3.1	154.1	3.3	2.8	1.3	3.6	11.0	165.5
	200	0.2	160.1	6.9	6.0	2.5	8.6	24.0	184.1
For 24.0 GHz	10	23.6	140.1	1.2	1.7	0.3	0.4	3.6	143.7
	50	6.2	154.1	6.8	8.8	1.7	2.8	20.1	174.2
	100	3.1	160.1	13.5	17.8	3.3	4.6	39.2	199.3
	200	0.2	166.1	27.0	35.0	6.7	13.5	82.2	248.3